

Multi-Brain Collaborative Control for Quadruped Robots

Anonymous Author(s)

Affiliation

Address

email

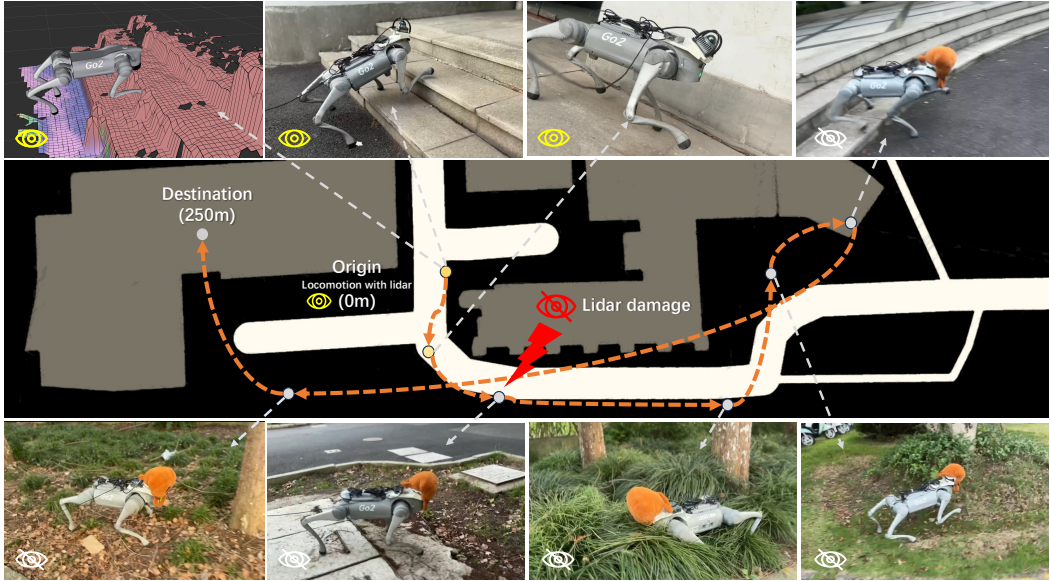


Figure 1: We conducted a long-distance (250m) test on a controller based on multi-brain collaborative. At the beginning of the map, the robot relied on height-map and proprioception to traverse through terrain. During the test, we simulated a scenario where the lidar suddenly malfunctioned (by covering it with a orange bag). The robot did not experience any mode crashes and was still able to handle complex terrains effectively.

1 **Abstract:** In the field of locomotion task of quadruped robots, Blind Policy and
2 Perceptive Policy each have their own advantages and limitations. The Blind Pol-
3 icy relies on preset sensor information and algorithms, suitable for known and
4 structured environments, but it lacks adaptability in complex or unknown environ-
5 ments. The Perceptive Policy uses visual sensors to obtain detailed environmental
6 information, allowing it to adapt to complex terrains, but its effectiveness is lim-
7 ited under occluded conditions, especially when perception fails. Unlike the Blind
8 Policy, the Perceptive Policy is not as robust under these conditions. To address
9 these challenges, we propose a Multi-Brain collaborative system that incorporates
10 the concepts of Multi-Agent Reinforcement Learning and introduces collaboration
11 between the Blind Policy and the Perceptive Policy. By applying this multi-policy
12 collaborative model to a quadruped robot, the robot can maintain stable locomo-
13 tion even when the perceptual system is impaired or observational data is incom-
14 plete. Our simulations and real-world experiments demonstrate that this system
15 significantly improves the robot’s passability and robustness against perception
16 failures in complex environments, validating the effectiveness of multi-policy col-
17 laboration in enhancing robotic motion performance.

18 **Keywords:** Quadruped Robots, Perception Fails, Multi-Brain Collaborative

19 **1 Introduction**

20 What happens if a robot suddenly loses its perception? Can it maintain its previous stable motion?
21 In natural environments, the sensory systems of humans and animals can sometimes experience
22 temporary or permanent impairments, such as “dark adaptation” phenomenon when moving from a
23 bright to a dark environment. In these situations, humans and animals can rely on past experiences
24 to immediately switch to a state of motion without sensory input, ensuring safe movement.

25 For humans, this ability stems from two main sources. First, the human brain has a strong adaptive
26 and memory capacity. When the perceptual system fails for a short period of time, the brain
27 will automatically call upon memories and experiences to compensate for the perceptual deficit.
28 Secondly, the human motor control system has a high degree of redundancy and multisensory integration.
29 For example, when vision fails, the proprioceptive and vestibular systems enhance their
30 role in maintaining balance movement.

31 In the motion tasks of bipedal and quadrupedal robots, sensory systems may fail due to incomplete
32 information or hardware malfunctions. These robots rely on various sensors to gather environmental
33 data, such as LiDAR, cameras, and ultrasonic sensors. However, the effectiveness of these sensors
34 can be limited in low-light or adverse weather conditions, or they may fail due to physical damage
35 or signal disruptions. Therefore, researching how to maintain stable robot motion under these
36 unfavorable conditions is a challenge in current studies.

37 In locomotion tasks, blind policies and perceptive policies each have their advantages and limitations [1]. Blind policies rely on sensors and preset algorithms for movement, requiring no visual
38 input [2, 3, 4, 5]. Although they are fast and consume fewer resources, their adaptability in complex or unknown environments is limited, and they have weaker obstacle recognition abilities and
41 generalizability. Perceptive policies use visual sensors to obtain detailed information about the environment, enabling robots to adapt to complex terrains [6, 7, 8]. However, in less than ideal visual
43 conditions or in known and structured environments, perceptive policies may not be as efficient as
44 blind policies. Researching how to effectively merge these two policies to cope with complex and
45 changing environments is an equally challenging research issue.

46 Addressing the challenges mentioned, this study integrates Multi-Agent Reinforcement Learning (MARL) [9, 10] to propose the concept of Multi-Brain Game Collaboration. We envision a
47 quadruped robot system integrating multiple policies to form a collective “brain” with each policy
49 tailored to different input policies. Specifically, we explore the interaction between a Blind
50 Policy, independent of perceptual input, and a Perceptive Policy that utilizes external information.
51 This model excels in scenarios with incomplete observational data or impaired sensory capabilities,
52 accurately simulating and analyzing the robot’s interactions with its environment. This approach
53 enhances decision-making and adaptability in complex environments.

54 The primary contributions of this research are as follows:

- 55 • **A Novel Multi-Brain Game Collaboration System:** This study introduces and successfully implements a multi-brain game collaboration system. In this system, each policy or “brain” independently and collaboratively optimizes decisions for different tasks. This design mimics the division of labor and cooperation in biological neural systems, significantly enhancing decision-making efficiency and precision.
- 60 • **Integration of Blind and Perceptive Policies:** The research thoroughly analyzes the combination of Blind Policies with Perceptive Policies. This collaborative policy provides an innovative approach for flexible movement in complex environments.
- 63 • **Enhanced Mobility in Complex Environments:** Through the non-zero-sum game [11] between blind and perceptive policies, this policy allows the robot to make accurate and effective motion decisions, even with incomplete information or limited perception.

66 **2 Related work**

67 **Multi-Agent Reinforcement Learning** In the field of Multi-Agent Reinforcement Learning
68 (MARL), there are generally three learning paradigms: centralized learning, independent learning,
69 and Centralized Training with Decentralized Execution (CTDE) [12]. Among these, CTDE effec-
70 tively combines the advantages of centralized learning with the flexibility of decentralized execution

71 MADDPG [13] is a typical representative of the CTDE paradigm, employing an actor-critic frame-
72 work. However, as an off-policy algorithm, MADDPG requires extensive memory storage to save
73 previous experiences and may not perform as stably in dynamic environments as on-policy algo-
74 rithms. MATD3 [14], a multi-agent version of TD3, enhances the stability of multi-agent cooper-
75 ation through double Q-learning and delayed policy updates, but this also increases computational
76 complexity, especially in large-scale multi-agent environments, and is extremely sensitive to hy-
77 perparameters, which may require extensive tuning and experimentation in practical applications to
78 achieve optimal performance.

79 MAPPO [15], for the first time, effectively extends the single-agent PPO algorithm to a multi-
80 agent environment, becoming an on-policy strategy that can handle complex multi-agent collabo-
81 rations while maintaining the stability and efficiency of policy updates. MAPPO not only retains
82 the advantages of PPO but also successfully addresses the collaboration problems in multi-agent
83 environments. Its application on the SMAC platform demonstrates its high sample efficiency and
84 consistency of policies [16].

85 **Blind Policy & Perceptive Motion Policy** In enhancing the adaptability and motion performance
86 of quadruped robots in complex environments, current research explores three primary policies. The
87 first policy, termed the blind policy, relies on the robot’s proprioceptive history, primarily utilizing
88 forelimb probing, to estimate terrain [3, 5, 2]. This policy faces limitations in complex or unknown
89 environments due to its weak obstacle recognition and generalization capabilities. The second policy
90 uses a holistic control approach based on external sensory inputs to gather environmental details,
91 helping the robot plan movements and navigate complex terrains [17, 18, 19, 20, 21]. However, this
92 often involves isolated end-to-end network architectures without testing for sensor reliability. The
93 third, a composite policy [22, 23] integrates blind and visual policies into a synergistic mechanism,
94 quickly adapting to sudden failures in external perception systems.

95 In sim2real applications for vision-based motion controllers using reinforcement learning, two main
96 approaches are prevalent: end-to-end training with depth or RGB images, effective in quadrupedal
97 robots, and using elevation maps [24, 25] or height scans from a Global Reference Frame. The latter
98 provides precise terrain information, enhancing adaptability and performance in complex environ-
99 ments. Compared to traditional images, elevation maps mitigate poor visual conditions, improving
100 navigation and decision-making [26, 27]. Furthermore, LiDAR offers high precision and reliability
101 under low light or visual occlusion, with its point cloud data converted into elevation maps providing
102 rich 3D terrain details, crucial for obstacle detection and terrain analysis.

103 To the best of the authors’ knowledge, there has been no research combining multi-agent reinfor-
104 cements learning algorithms such as MAPPO to achieve non-zero-sum games between blind policies
105 and perceptive policies. Our approach can accurately simulate and analyze the complex interactions
106 between the robot and the environment, even under conditions of incomplete observation data or
107 sensory loss, thereby enhancing the robot’s motion performance in various environments.

108 **3 Method**

109 **3.1 Task Formulation**

110 In the locomotion task of a quadruped robot, we define a process that combines a blind policy and
111 an external perception-based policy to handle complex environments. Specifically, the quadruped
112 robot can flexibly navigate various obstacles such as highlands, gaps, obstacles, and stairs when

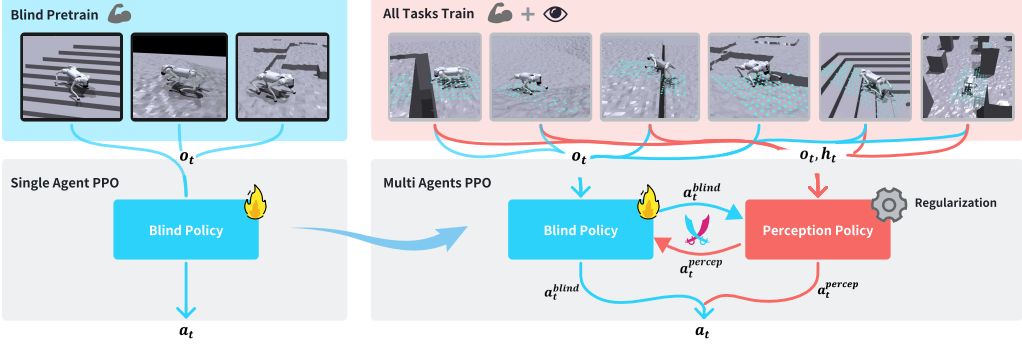


Figure 2: Two-stage multi-brain game collaborative training framework.

113 external perception (e.g., LiDAR elevation maps) is functioning properly. However, when external
 114 perception suddenly fails, the quadruped robot, although unable to navigate terrains such as gaps,
 115 should still retain the capability to traverse complex terrains like stairs and ramps.

116 We have designed a two-stage training approach, as illustrated in Figure 2. In the first stage, a
 117 training mode without external perception is used, involving only a blind policy. In the second
 118 stage, a multi-agent approach is employed, incorporating external perception and simultaneously
 119 training both the blind policy and a perceptive policy with perception capabilities. The collaboration
 120 between these two policies is guided by a terrain reconstruction error regularization term. This
 121 ensures that our robot can effectively traverse terrains both with and without perception.

122 3.2 Base Set

123 **Theorem** In complex 3D environments, quadruped robots must maintain stable navigation and
 124 locomotion even when external perception capabilities fail. To achieve this objective, we describe
 125 the locomotion problem of quadruped robots using a Partially Observable Markov Decision Process
 126 (POMDP) [28, 29].

127 The POMDP framework effectively models decision-making scenarios where information is incom-
 128 plete, defining key elements such as states, actions, observations, and rewards. In this model, the
 129 environment at time step t is represented by a complete state x_t . Based on the agent’s policy, an
 130 action a_t is performed, resulting in a state transition to x_{t+1} with a probability $P(x_{t+1} | x_t, a_t)$. The agent
 131 then receives a reward r_t and a partial observation o_{t+1} . The aim of reinforcement learning
 132 here is to identify a policy π that maximizes the expected discounted sum of future rewards:

$$J(\pi) = \mathbb{E}_\pi \left[\sum_{t=0}^{\infty} \gamma^t r_t \right]$$

133 **Action Space & State Space** The action spaces for the blind policy and perceptive policy are
 134 respectively $a_t^{blind} \in \mathbb{R}^{12}$ and $a_t^{percep} \in \mathbb{R}^{12}$, representing the offset from the default pos-
 135 ition for each joint. The critic networks for both policies observe the global state $s_t^{critic} =$
 136 $[o_t, v_t, e_t, h_t, a_t^{percep}, a_t^{blind}]^T$, which includes proprioceptive observations o_t , estimated linear
 137 velocities \hat{v}_t , and latent variables e_t such as body mass, center of mass position, friction coefficients,
 138 and motor strength. These global observations are crucial for the second phase of training, helping
 139 the critic network make balanced decisions during the interactions between the two policies and
 140 preventing training collapse due to excessive competition.

141 For the actor networks, the state space for the blind policy includes proprioceptive observations
 142 o_t , estimated linear velocity \hat{v}_t , and latent variables e_t . Additionally, aligning with the multi-agent
 143 game theory approach, the state space for the blind policy also incorporates the output from the
 144 Perceptive Policy a_t^{percep} , expressed as $s_t^{blind} = [o_t, \hat{v}_t, e_t, a_t^{percep}]^T$. Similarly, the state space

145 for the Perceptive Policy is $s_t^{percep} = [o_t, h_t, a_t^{blind}]^T$, where h_t represents the local elevation map
146 centered around the robot.

147 During the first phase of training for the Blind policy, we employed the Regularized Online Adap-
148 tation (ROA) method [30] to estimate the explicit observations \hat{v}_t and the latent variables e_t . In this
149 phase, a_t^{percep} was set to zero. In the second phase of training, the final action $a_t = a_t^{percep} + a_t^{blind}$.

150 **3.3 First Stage**

151 In the first stage of training, we primarily developed a proprioceptive motion system for the
152 quadruped robot, aimed at enabling the robot to traverse various complex terrains such as uneven
153 slopes, stairs, and discrete terrains without direct visual or elevation map input to the policy. During
154 this phase, the output action item for the perception policy was set as a 12-dimensional zero vector,
155 ensuring that the blind policy operates without interference from other agents' outputs. Our blind
156 policy, inspired by the ROA training framework, uses only current proprioceptive inputs and the
157 action outputs of other agents at time t to estimate the robot's real-time privileged information, such
158 as speed. This approach does not require a long temporal window, allowing the network to estimate
159 the robot's state based solely on its current status and actions. Additionally, the training utilized an
160 asymmetric Actor-Critic structure to better evaluate the quality of the actions output by the Actor.

161 For the robot's elevation map, we trained a Variational Autoencoder (VAE) model primarily to mem-
162 orize the terrains encountered by the blind policy and to compute regularization terms for action
163 constraints in the subsequent training phase.

164 **3.4 Second Stage**

165 In the second stage of learning, we introduced a multi-agent learning approach, utilizing a non-zero-
166 sum game strategy to optimize the external perception controllers for quadruped robots. Unlike
167 traditional single-policy approaches such as parkour, this method allows for adaptation when one
168 controller fails, as other controllers can detect and adjust their actions, enhancing the system's ro-
169 bustness. Within the multi-agent framework, the gradients for each controller are updated indepen-
170 dently, facilitating task separation and allowing each controller to focus on specific tasks, thereby
171 improving the overall adaptability of the system. Additionally, this model supports "hot-swapping"
172 of the perception system, enabling the robot to move based on sensory data when available and to
173 continue proprioceptive movement without malfunction when perception is unexpectedly lost.

174 The primary implementation policy is as follows: initially, load the pre-trained model of the single-
175 agent blind policy and activate these models in the second phase to utilize the actual outputs from
176 the perceptive policy. Inputs to the perceptive policy include proprioceptive data, outputs from the
177 blind policy, and elevation map information, primarily adjusted for terrain. The robot's final actions
178 are a combination of perceptive and blind actions. This framework ensures that during training, the
179 perceptive and blind policies interact and collaborate to optimize movement. All networks use the
180 CTDE approach with MAPPO [15] updates, where each agent's Critic network shares all environ-
181 mental information, including the inputs and outputs of other agents, during training, while each
182 operates independently during execution. The loss calculations and updates for the blind policy
183 remain as in the first phase, while the perceptive policy's loss includes surrogate loss, value loss,
184 entropy loss, and a Reconstruction Error Regularizer. The purpose of the regularization term is to
185 encourage the Percep policy to minimize actions when encountering terrain similar to those han-
186 dled by the blind policy, promoting cooperation between the two policies and reducing excessive
187 competition.

188 **3.5 VAE & Perception Cooperation Constraint Regularization**

189 In the first stage, we primarily trained the quadruped robot to navigate slopes, steps, and discrete
190 obstacles without relying on external perception. These terrains were chosen because they enable
191 the robot to learn fundamental locomotion skills and develop robust capabilities. Steps, in particular,

192 significantly improve the robot’s ability to lift its legs and react to tripping, thereby enhancing overall
193 mobility. We believe these terrains exemplify the types of environments a robot can navigate without
194 perception in real-world scenarios. We designed a Variational Autoencoder (VAE) to encode and
195 decode these features, with the VAE being updated using MSE and KL divergence during the first
196 stage.

197 In the second stage, we introduced more challenging terrains, such as highlands, gaps, and pillars,
198 which are difficult for the robot to navigate using only the Blind Policy trained in the first
199 stage. Therefore, it must rely on the Percep policy with external perception input for compensation.
200 However, the complexity introduced by Multi-Agent systems can lead to policies converging
201 to local optima, with the blind policy and Percep policy potentially competing against each other,
202 hindering coordinated control. To address this, we introduced a perception cooperation constraint
203 regularization term based on elevation maps. This term helps ensure that if the current elevation
204 map reconstruction error, as produced by the VAE, is below a threshold, indicating familiarity with
205 the terrain, the regularization term increases with the Percep policy’s output, limiting its action. If
206 the reconstruction error exceeds the threshold, indicating unfamiliar terrain, the regularization term
207 is set to zero, encouraging the Percep policy to compensate.

208 Specifically, in the second stage, the robot’s current elevation map h_{ij} is input into the VAE,
209 which reconstructs the elevation map \hat{h}_{ij} . The reconstruction error is then calculated as $E_i =$
210 $\frac{1}{n} \sum_{j=1}^n (\hat{h}_{ij} - h_{ij})^2$, where i represents the i -th sample in the batch, j represents the index of the
211 dimensions of the elevation map and action, and n represents the dimension of the elevation map.
212 Based on the reconstruction error and the threshold, we define the penalty factor:

$$\mathbb{I}_i = \begin{cases} 0 & \text{if } E_i > \tau \\ 1 & \text{if } E_i \leq \tau \end{cases}$$

213 This means that when the reconstruction error exceeds the threshold, the regularization term is set
214 to 1, otherwise it is 0. The perception cooperation constraint regularization term is then introduced
215 as:

$$\mathcal{P}_i = \frac{1}{m} \sum_{i=1}^m \mathbb{I}_i \sum_{j=1}^k a_{ij}^2$$

216 where k represents the dimension of the action, and m represents the batch size. Finally, the to-
217 tal loss function consists of the surrogate loss, value function loss, policy entropy, and the action
218 regularization term:

$$\mathcal{L} = \mathcal{L}_{\text{surrogate}} + \lambda_v \mathcal{L}_{\text{value}} - \lambda_e \mathcal{H}(\pi) + \lambda_a \mathcal{P}_i$$

219 4 Experimental Results

220 4.1 Experiment Setup

221 We used the Unitree Go2 robot as our experimental subject, which features 12 degrees of freedom
222 in its legs. Utilizing a single NVIDIA RTX 4090 GPU, we simultaneously trained 4096 domain-
223 randomized Go2 robot environments in Isaac Gym. During training, we employed PD position
224 controllers for each joint, with both the Blind Policy and Perception Policy running at a frequency
225 of 50 Hz. The elevation map update rate was set to 10 Hz, and the robot’s control signal delay
226 was 20 ms. Additional domain randomization parameters and training specifics are detailed in the
227 appendix.

228 The training terrain comprised six types: ramps, stairs, discrete obstacles, highlands, gaps, and pillar
229 terrain. The first three terrains are relatively easier for the robot to navigate, while the last three
230 require more reliance on external perception for anticipation. We primarily measured the robot’s
231 performance in both simulated and real-world settings under two conditions:

- 232 • The robot’s ability to navigate the tough terrains with the aid of perception.
233 • The robot’s capability to traverse the first three terrains when perception is suddenly lost.

234 **4.2 Simulation Experiment**

235 **Terrain Passability Experiment:** We first tested the survival rate of our policy across three tough
 236 terrains with varying levels of difficulty. For each terrain and difficulty level, we conducted 100
 237 environment samples, calculated the success rate four times, and averaged the results. The success
 238 rate for the Gap and Pit terrains was defined as the robot successfully crossing or climbing over
 239 the obstacle, while for the Pillar terrain, it was defined as the proportion of environments the robot
 240 navigated without collisions. As shown in Table 1 , our policy achieved high success rates across
 241 various tough terrains. The highest difficulty level for each terrain was beyond the scope of our
 curriculum settings, demonstrating the robustness of our algorithm.

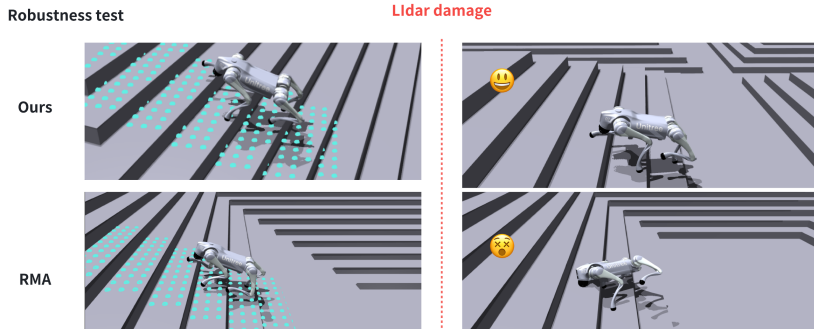


Figure 3: Robustness testing In simulation, the perception-based RMA mode collapses when the height map is corrupted while our policy works well.

Gap	Success Rate	Pit	Success Rate	Pillar	Success Rate
0.35m	99.3%	0.30m	97.6%	obstacle size=0.4 ; distance=1.6	86.7%
0.45m	98.3%	0.40m	97.6%	obstacle size=0.5 ; distance=1.5	80.4%
0.55m	91.3%	0.50m	85.0%	obstacle size=0.6 ; distance=1.4	65.0%
0.65m	44.3%	0.55m	49.3%	obstacle size=0.7 ; distance=1.3	60.7%

Table 1: Success Rates in Tough Terrains

243 **Comparison Experiment:** We compared our collision estimation and response policy with several
 244 baselines and ablations as follows:

- 245 • **Baseline:** Training directly with proprioception and height map.
- 246 • **RMA:** Employing an Adaptation Module to estimate all privileged observations, but di-
 247 rectly inputting the elevation map into proprioception.
- 248 • **Ours w/o Regularizer:** Training without Perception Cooperation Constraint Regulariza-
 249 tion.

250 As shown in Table 2, our method demonstrates the most robust performance under external per-
 251 ception failure, especially when climbing stairs. Other strategies failed to learn to handle obstacles
 252 without perception during training, resulting in tripping over obstacles. In contrast, our method can
 253 easily climb steps, and the MXD indicates that our method can also achieve higher speeds (1 m/s to
 254 1.6 m/s). Figure 3. shows the effect of our run in simulation.

255 **4.3 Physical Experiments**

256 **Navigating Complex Terrains with Sensory Input** Our policy substantially enhanced the
 257 quadruped robot’s capability to navigate vertical challenges, such as wooden boxes and low walls.
 258 In our experiments, the robot was tasked with climbing a 32 cm high wooden box. It adeptly lifted
 259 its front legs preemptively and elevated its body to surmount the box, as shown in Figure 4. This
 260 sequence of movements, successfully culminating in the robot climbing over the box, exemplifies

Method	Up Stair Success	Down Stair Success	Discrete Success	Stair XMD	Discrete XMD
Ours	97%	100%	90%	19.97	17.04
RMA	0%	100%	81%	8.2	12.38
Baseline	0%	100%	76%	7.8	11.53
Ours w/o VAE	87%	100%	90%	16.42	14.99

Table 2: we primarily compared the success rates of different methods on stairs and discrete terrains, as well as the Mean X-Displacement (XMD) for each environment. For this experiment, all elevation map inputs were set to zero, and we tested 1048 environments over 1000 steps. The stairs had a width of 0.31 and a height of 0.13, while the maximum height of the discrete terrain was 0.15. Failure conditions were defined as either the roll or pitch exceeding 1.3, or the robot’s foot getting stuck and unable to move forward.

261 the efficacy of our integrated elevation map and perceptual policies in enabling the robot to tackle
 262 climbing obstacles.



Figure 4: Robot Climbing a Wooden Box Using Our Policy.

263 In the obstacle avoidance trials, the robot encountered various obstacles including rocks, wooden
 264 boxes, and human figures. Leveraging our policy, it quickly recognized a human-shaped obstacle
 265 through its elevation map, then adeptly adjusted its trajectory, sidestepping to bypass the obstacle
 266 efficiently and safely, as depicted in Figure 5. This performance underscores our method’s effective-
 267 ness, particularly noting that despite the absence of y-direction velocity training, the robot adeptly
 268 maneuvered in the y-direction, showcasing the robustness and adaptability of our approach.

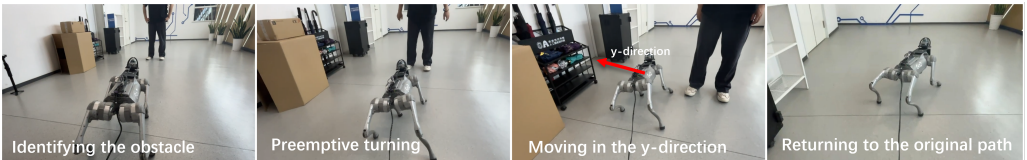


Figure 5: Robot Avoiding a Person Using Our Policy.

269 **Long-Distance Test with Outdoor Terrain Perception Failure** Initially, with effective LiDAR
 270 elevation map inputs, the robot used a comprehensive policy for movement, efficiently climbing
 271 16 cm stairs and handling slopes. Subsequently, we deliberately covered the LiDAR, disabling the
 272 elevation map input, and conducted a long-distance test on unstructured terrains. We tested the
 273 robot over a 250m path that included dense grass, irregular terrain, soft and slippery grasslands,
 274 gentle slopes, and stair terrains, where the robot successfully navigated through all (see Figure 1).

275 5 Conclusion, Limitations and Future Directions

276 We propose the concept of Multi-Brain Collaborative Control based on Multi-Agent systems, estab-
 277 lishing a training framework that achieves both perceptive motion and robust obstacle traversal in the
 278 event of perception failure. We tested our system in both simulations and real-world experiments,
 279 demonstrating the effectiveness and robustness of our algorithm. However, currently, our robot’s
 280 elevation maps are derived from LiDAR, which heavily depends on the frequency and stability of
 281 the odometry, and involves significant computational overhead. This greatly affects the stability and
 282 sustainability of our perceptive policy. Additionally, our perceptive algorithm is still quite sensitive
 283 to environmental noise. In the future, we aim to replace LiDAR with lighter-weight perception de-
 284 vices such as cameras and construct local elevation maps without relying on odometry. We will also
 285 explore how to apply our algorithm to control various legged robots.

286 **References**

- 287 [1] M. T. Shahria, M. S. H. Sunny, M. I. I. Zarif, J. Ghommam, S. I. Ahamed, and M. H. Rah-
288 man. A comprehensive review of vision-based robotic applications: Current state, components,
289 approaches, barriers, and potential solutions. *Robotics*, 11(6):139, 2022.
- 290 [2] I. M. A. Nahrendra, B. Yu, and H. Myung. Dreamwaq: Learning robust quadrupedal lo-
291 comotion with implicit terrain imagination via deep reinforcement learning. In *2023 IEEE
292 International Conference on Robotics and Automation (ICRA)*, pages 5078–5084. IEEE, 2023.
- 293 [3] J. Lee, J. Hwangbo, L. Wellhausen, V. Koltun, and M. Hutter. Learning quadrupedal locomo-
294 tion over challenging terrain. *Science robotics*, 5(47):eabc5986, 2020.
- 295 [4] Y. Cheng, H. Liu, G. Pan, L. Ye, H. Liu, and B. Liang. Quadruped robot traversing 3d complex
296 environments with limited perception, 2024.
- 297 [5] J. Siekmann, K. Green, J. Warila, A. Fern, and J. Hurst. Blind bipedal stair traversal via sim-
298 to-real reinforcement learning. *arXiv preprint arXiv:2105.08328*, 2021.
- 299 [6] Y. D. Yasuda, L. E. G. Martins, and F. A. Cappabianco. Autonomous visual navigation for
300 mobile robots: A systematic literature review. *ACM Computing Surveys (CSUR)*, 53(1):1–34,
301 2020.
- 302 [7] P. Fankhauser, M. Bjelonic, C. D. Bellicoso, T. Miki, and M. Hutter. Robust rough-terrain
303 locomotion with a quadrupedal robot. In *2018 IEEE International Conference on Robotics
304 and Automation (ICRA)*, pages 5761–5768. IEEE, 2018.
- 305 [8] P. Fankhauser. *Perceptive locomotion for legged robots in rough terrain*. PhD thesis, ETH
306 Zurich, 2018.
- 307 [9] D. Huh and P. Mohapatra. Multi-agent reinforcement learning: A comprehensive survey. *arXiv
308 preprint arXiv:2312.10256*, 2023.
- 309 [10] S. Gronauer and K. Diepold. Multi-agent deep reinforcement learning: a survey. *Artificial
310 Intelligence Review*, 55(2):895–943, 2022.
- 311 [11] D. B. Gillies. Solutions to general non-zero-sum games. *Contributions to the Theory of Games*,
312 4(40):47–85, 1959.
- 313 [12] C. Zhu, M. Dastani, and S. Wang. A survey of multi-agent reinforcement learning with com-
314 munication. *arXiv preprint arXiv:2203.08975*, 2022.
- 315 [13] R. Lowe, Y. I. Wu, A. Tamar, J. Harb, O. Pieter Abbeel, and I. Mordatch. Multi-agent actor-
316 critic for mixed cooperative-competitive environments. *Advances in neural information pro-*
317 *cessing systems*, 30, 2017.
- 318 [14] J. Ackermann, V. Gabler, T. Osa, and M. Sugiyama. Reducing overestimation bias in multi-
319 agent domains using double centralized critics. *arXiv preprint arXiv:1910.01465*, 2019.
- 320 [15] C. Yu, A. Velu, E. Vinitsky, J. Gao, Y. Wang, A. Bayen, and Y. Wu. The surprising effectiveness
321 of ppo in cooperative multi-agent games. *Advances in Neural Information Processing Systems*,
322 35:24611–24624, 2022.
- 323 [16] J. Hu, S. Hu, and S.-w. Liao. Policy regularization via noisy advantage values for cooperative
324 multi-agent actor-critic methods. *arXiv preprint arXiv:2106.14334*, 2021.
- 325 [17] T. Miki, J. Lee, J. Hwangbo, L. Wellhausen, V. Koltun, and M. Hutter. Learning robust per-
326 ceptive locomotion for quadrupedal robots in the wild. *Science Robotics*, 7(62):eabk2822,
327 2022.

- 328 [18] W. Yu, D. Jain, A. Escontrela, A. Iscen, P. Xu, E. Coumans, S. Ha, J. Tan, and T. Zhang. Visual-
329 locomotion: Learning to walk on complex terrains with vision. In *5th Annual Conference on*
330 *Robot Learning*, 2021.
- 331 [19] C. Mastalli, I. Havoutis, M. Focchi, D. G. Caldwell, and C. Semini. Motion planning for
332 quadrupedal locomotion: Coupled planning, terrain mapping, and whole-body control. *IEEE*
333 *Transactions on Robotics*, 36(6):1635–1648, 2020.
- 334 [20] A. Agarwal, A. Kumar, J. Malik, and D. Pathak. Legged locomotion in challenging terrains
335 using egocentric vision. In *Conference on robot learning*, pages 403–415. PMLR, 2023.
- 336 [21] Z. Zhuang, Z. Fu, J. Wang, C. Atkeson, S. Schwertfeger, C. Finn, and H. Zhao. Robot parkour
337 learning. *arXiv preprint arXiv:2309.05665*, 2023.
- 338 [22] H. Duan, B. Pandit, M. S. Gadde, B. J. van Marum, J. Dao, C. Kim, and A. Fern. Learning
339 vision-based bipedal locomotion for challenging terrain. *arXiv preprint arXiv:2309.14594*,
340 2023.
- 341 [23] Z. Fu, A. Kumar, A. Agarwal, H. Qi, J. Malik, and D. Pathak. Coupling vision and proprioception
342 for navigation of legged robots. In *Proceedings of the IEEE/CVF Conference on Computer*
343 *Vision and Pattern Recognition*, pages 17273–17283, 2022.
- 344 [24] P. Fankhauser, M. Bloesch, C. Gehring, M. Hutter, and R. Siegwart. Robot-centric elevation
345 mapping with uncertainty estimates. In *Mobile Service Robotics*, pages 433–440. World Scientific,
346 2014.
- 347 [25] T. Miki, L. Wellhausen, R. Grandia, F. Jenelten, T. Homberger, and M. Hutter. Elevation map-
348 ping for locomotion and navigation using gpu. In *2022 IEEE/RSJ International Conference on*
349 *Intelligent Robots and Systems (IROS)*, pages 2273–2280. IEEE, 2022.
- 350 [26] P. Fankhauser, M. Bloesch, and M. Hutter. Probabilistic terrain mapping for mobile robots
351 with uncertain localization. *IEEE Robotics and Automation Letters*, 3(4):3019–3026, 2018.
- 352 [27] M. Stölzle, T. Miki, L. Gerdes, M. Azkarate, and M. Hutter. Reconstructing occluded elevation
353 information in terrain maps with self-supervised learning. *IEEE Robotics and Automation*
354 *Letters*, 7(2):1697–1704, 2022.
- 355 [28] G. Shani, J. Pineau, and R. Kaplow. A survey of point-based pomdp solvers. *Autonomous*
356 *Agents and Multi-Agent Systems*, 27:1–51, 2013.
- 357 [29] M. T. Spaan and N. Spaan. A point-based pomdp algorithm for robot planning. In *IEEE*
358 *International Conference on Robotics and Automation, 2004. Proceedings. ICRA'04. 2004*,
359 volume 3, pages 2399–2404. IEEE, 2004.
- 360 [30] Z. Fu, X. Cheng, and D. Pathak. Deep whole-body control: Learning a unified policy for
361 manipulation and locomotion. In *Conference on Robot Learning*, pages 138–149. PMLR,
362 2023.